THE JOURNAL OF PHYSICAL CHEMISTRY Letters

Letter

pubs.acs.org/JPCL

Recombination Study of Combined Halides (Cl, Br, I) Perovskite Solar Cells

Belen Suarez,[†,‡] Victoria Gonzalez-Pedro,[†] Teresa S. Ripolles,[†] Rafael S. Sanchez,[†] Luis Otero,[‡] and Ivan Mora-Sero*[,†]

[†]Photovoltaics and Optoelectronic Devices Group, Departament de Física, Universitat Jaume I, 12071 Castelló, Spain

[‡]Departamento de Química, Universidad Nacional de Río Cuarto, Agencia Postal No 3, X5804BYA Río Cuarto, Argentina

Supporting Information

ABSTRACT: We report on the preparation of a series of solution-processed perovskite solar cells based on methylammonium (MA) lead halide derivatives, $MAPbX_3$, which show tunable optical properties depending on the nature and ratio of the halides employed (X = Cl, Br, and I). Devices have been prepared with different cell architecture, thin film, and mesoporous scaffold (TiO_2 and Al_2O_3). We have analyzed different sample sets focusing on the characterization of the charge recombination by means of impedance spectroscopy (IS). On the one hand, our study discloses that the insertion of both Cl and Br in the perovskite lattice reduces the charge recombination rates in the light absorber film, thus determining the open circuit voltage (V_{oc}) of the device. The samples prepared on a mesoporous Al_2O_3 electrode present lower charge recombination rates than those devices prepared on mesoporous TiO_2. Furthermore, the addition of Br in the perovskite structure was demonstrated to improve slightly the lifetime of the devices; in fact, the efficiencies of all devices tested remained at least at the 80% of the initial value 1 month after their preparation. These results highlight the crucial role of the charge-recombination processes on the performance of the perovskite solar cells and pave the way for further progress on this field.

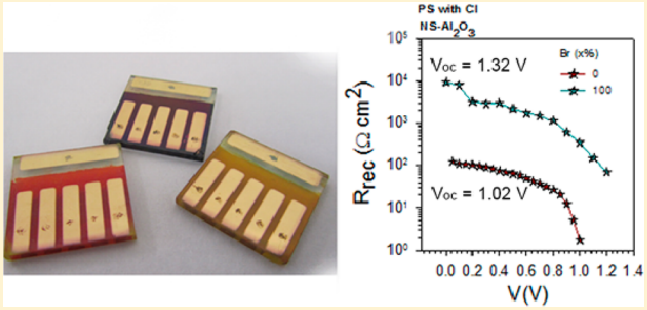

SECTION: Energy Conversion and Storage; Energy and Charge Transport

Hybrid lead halide perovskite solar cells have revolutionized justifiably the photovoltaic technology for several reasons: the demonstration of efficiencies as high as 15 to 16%,[1−5] the possibility of preparing the devices by solution techniques at low temperatures,[6,7] and, consequently, the low-cost production and the compatibility with flexible substrates, which widen its versatility.[8,9] Moreover, the generic perovskite (PS) structure ABX_3 allows manufacturing a broad range of different PS materials by simple modification of the building blocks A, B, and X; nonetheless, the ionic radii ratios of the different constituents seem to play a role in the formation of the PS structure and its properties.[6,10,11] To date, the highest efficiency reported on PS solar cells corresponds to materials bearing A = methylammonium (MA), B = Pb, and X = I or I with traces of Cl.[1−4] However, the recently achieved efficiencies higher than 14% based on formamidinium instead of MA prove the versatility of the PS materials for the photovoltaic technology.[12] Additionally, the use of Br instead of I produces a PS material with broader band gap.[13−15] In fact, it is possible to tailor the $MAPbX_3$ band gap from 1.57 to 2.29 eV by changing the ratio of I and Br ($X = Br_xI_{1-x}$, x ranges from 0 to 1).[12,15] The simplicity of tuning the optical properties of the PS-based materials makes them extraordinary appealing for the development of tandem solar cells, where the light absorption ability of the different layers must not overlap with the aim of harvesting photons in a wider range of the solar spectrum, thus achieving higher power conversion efficiencies.[7,14]

Despite the outstanding results obtained for the PS photovoltaic devices in the last 2 years, the physical mechanisms that rule the cell performance are not yet fully understood. For instance, it is still unclear why solar cells with a priori different device configurations, that is, thin film (without scaffold layer),[2,5,16] sensitized solar cell (mesoporous TiO_2 layer)[1,17] and meso-superstructured solar cell (mesoporous Al_2O_3 or ZrO_2 layers),[18−20] can achieve high efficiencies. Recently, we have observed that the charge carriers can be accumulated in the PS bulk,[18] regardless of using thin-film or mesoporous TiO_2 cell configuration. These results evidence a common working behavior,[21] which points to a characteristic performance of the PS-based solar cells. However, the charge diffusion length of the $MAPbI_3$ sample increases when a mesoporous TiO_2 film is used compared with the thin-film configuration.[21] Additionally, the use of $PbCl_2$ as lead source

Received: April 6, 2014
Accepted: April 17, 2014

   dx.doi.org/10.1021/jz5006797 | J. Phys. Chem. Lett. 2014, 5, 1628−1635

during the synthesis of $MAPbI_3$ also affects the properties of PS material.[14,19,22,23] In particular, the charge diffusion length observed for thin film $MAPbI_{3-y}Cl_y$ samples is longer than that for the $MAPbI_3$ derivatives.[24] It has been observed as well that holes can be extracted more efficiently than electrons from $MAPbI_3$.[22] Therefore, the use of Cl precursor during the PS synthesis takes an important role in the charge extraction processes. In conclusion, despite the great efforts focused on the understanding of the PS solar cells performance, many open questions remain to be explored.

The novelty of the PS solar cells accounts for the scarce knowledge on the physical fundamentals and mechanisms occurring during the photon to electron conversion. Although several works aimed at measuring physical constants, such as the lifetime[25−28] or the charge diffusion lengths,[21,24,29] can be found in the literature, up to our knowledge, no studies centered on the charge recombination processes for different PS composition and cell configuration have been carried out so far. In this work, we exploit and focused on the charge recombination of the PS-based photovoltaic devices because it directly influences on the photovoltaic parameters, having a special impact on the open circuit voltage, V_{oc}. Therefore, unraveling the charge recombination mechanisms and measuring the physical constants that rule them represent some of the key factors of the cell performance; hence, here we analyze the recombination resistance, R_{rec}, which is inversely proportional to the recombination rate.[30] Impedance spectroscopy (IS), which is a widely employed technique for characterizing photovoltaic devices,[30] allowed the determination of the R_{rec} of a series of PS-based devices and revealed unprecedented results.[3,8,18,21,31−34]

The effect of the different ratios of halides (Cl, Br, and I) and the influence of the cell configuration on the PS solar cells performance is investigated by means of a systematic analysis, in which several device architectures are evaluated, including thin-film and nanostructured electrodes (NS-TiO_2 and NS-Al_2O_3, depending on the scaffold material); all of these samples were prepared by the one-step methodology.[19,35] We systematically observed that those devices with lower recombination rates presented higher V_{oc} values, which drastically determines the cell performance. This work emphasizes on this fact relating the observed V_{oc} to recombination rate for a broad range of PS light-absorbing materials and cell configuration.

Detailed information on materials, device preparation, and characterization methods is provided at the Supporting Information. Perovskite samples are denoted as $MAPb(Br_xI_{1-x})_{3-y}Cl_y$, where x is determined by the ratio between Br and I precursors but y is not determined. The effect of Cl precursor in the PS synthesis is still controversial; just extremely reduced amounts of Cl have been detected in $MAPbI_{3-y}Cl_y$ or even have not been detected.[22,23] The exact effect of Cl in terms of changing the electrical properties or modifying the crystallinity of the PS is not known.[22] In this sense, we have use the notation $MAPb(Br_xI_{1-x})_{3-y}Cl_y$ for coherence with the most extended notation in the literature but just as an indicator of the use of Cl precursor in the PS synthesis.

A picture of complete PS photovoltaic devices prepared with a combination of the three halides in a different ratio, $MAPb(Br_xI_{1-x})_{3-y}Cl_y$, where $0 \le x \le 1$, is shown in Figure 1a. It can be appreciated at first sight how the color of the absorber films is tuned from dark brown to yellow by controlling the amount of Br. The absorption spectra of the

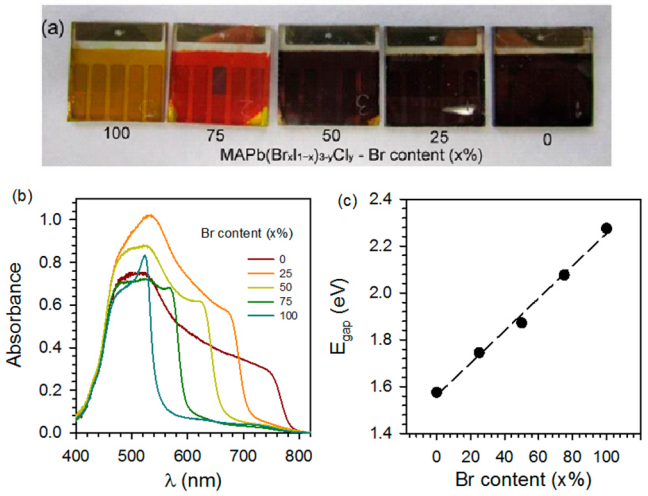

Figure 1. (a) Picture of $MAPb(Br_xI_{1-x})_{3-y}Cl_y$, $(0 \le x \le 1)$ devices with different Br/I molar ratios grown on mesoporous TiO_2 substrates after sample characterization. (Yellow parts in some samples indicate degradation.) (b) Absorption spectra of the samples (absorption tail observed at long wavelengths is due to the mesoporous layer light scattering). (c) The energy band gap extracted from the absorption measurements depending on the percentage of the Br.

mixed halide PS films were measured and are depicted in Figure 1b. A systematic shift of the absorption band edge to shorter wavelengths is observed with increasing the Br content. Therefore, the energy band gap (E_g) can be easily tuned by modifying the Br/I ratio. The energy gap values obtained from the intersection of the linear extrapolation of the absorption band edge with the horizontal axis are plotted in Figure 1c for those samples with different halide compositions. A linear dependence of the band gap with the Br content is observed, where $E_g = 1.563 + 6.916 \times 10^{3}\cdot[x]$, where $[x]$ is bromide percentage. It should be remarked that the E_g values obtained for $MAPbI_{3-y}Cl_y$ and $MAPbBr_{3-y}Cl_y$, 1.57 and 2.27 eV, are in good agreement with the previous works reported in the literature.[15,35,36] A similar trend is observed for films grown by one-step methodology onto mesoporous Al_2O_3 and PS films prepared without Cl. (See Figure SI1 in the Supporting Information.)

Perovskite solar cells with different halide compositions were prepared and characterized by measuring their current−voltage (J−V) characteristics. Figure 2 shows the averaged J−V curves for PS devices with different Br/I ratios under 1 sun illumination. The highest efficiency obtained under each condition as well as the average of photovoltaic parameters for a number "n" of PS devices are summarized in Table 1. The data include $MAPb(Br_xI_{1-x})_3$ solar cells grown onto NS-TiO_2 substrates and $MAPb(Br_xI_{1-x})_{3-y}Cl_y$ PS devices using NS-TiO_2 and NS-Al_2O_3 electrodes. It is observed that those samples prepared with Cl precursor (Figure 2b, c) present higher efficiencies than their counterparts without Cl (Figure 2a) independently of the Br/I ratios. This trend is due to an increase in both V_{oc} and short circuit current, J_{sc}, while fill factor (FF) is in the same range (see Table 1). On the contrary, a significant drop of the cell efficiency is observed by increasing the amount of Br due to a decrease in the J_{sc}, which is ascribed to the blue shift of the absorption band-edge (Figure 1b). Additionally, $MAPb(Br_xI_{1-x})_{3-y}Cl_y$ PS devices using NS-TiO_2 exhibit lower J_{sc} and significantly lower V_{oc} than devices prepared on NS-Al_2O_3 electrodes (see Figure 2b, c).

dx.doi.org/10.1021/jz5006797 | J. Phys. Chem. Lett. 2014, 5, 1628−1635

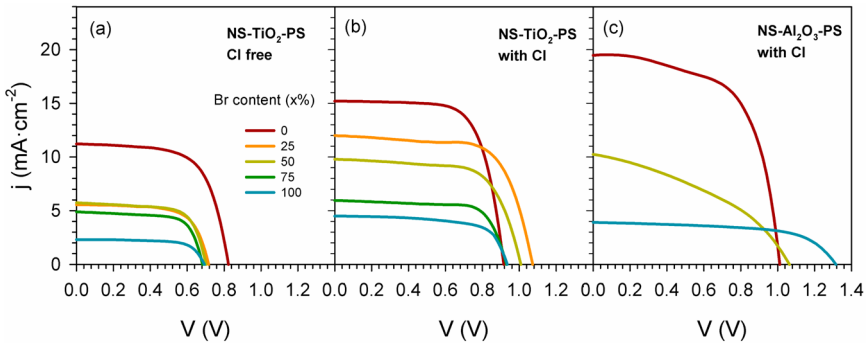

Figure 2. Average current−voltage curves under AM 1.5 solar irradiance and 100 mW cm^{-2} light intensity conditions of combining a mixture of halides PS with different Br/I molar ratios. Cl-free $MAPb(Br_xI_{1-x})_3$, $0 \le x \le 1$, on NS-TiO_2 substrates (a) and trihalide perovskites with a structure of $MAPb(Br_xI_{1-x})_{3-y}Cl_y$, $0 \le x \le 1$, on NS-TiO_2 (b) and NS-Al_2O_3 (c) substrates. Data plotted are the mean of $2 \le n \le 10$ working devices; see Table 1.

Table 1. Photovoltaic Parameters, Extracted from *J*−*V* Curves, of the PS Solar Cells Prepared with Different Combination of Halides (Cl, Br, I)[a]

	Br (x%)		J_{sc} (mA cm^{-2})	V_{oc} (V)	FF	η (%)	E_{gap} (eV)
NS-TiO_2	0		11.7	0.833	0.668	6.5	
$MAPb(Br_xI_{1-x})_3$		n = 8	11.22 ± 0.64	0.824 ± 0.02	0.652 ± 0.01	6.1 ± 0.4	
	25		5.87	0.716	0.680	2.9	
		n = 4	5.55 ± 0.30	0.719 ± 0.020	0.670 ± 0.012	2.7 ± 0.2	
	50		5.96	0.711	0.686	2.9	
		n = 10	5.74 ± 0.18	0.704 ± 0.025	0.683 ± 0.063	2.8 ± 0.1	
	75		5.70	0.718	0.685	2.8	
		n = 5	5.09 ± 0.35	0.688 ± 0.023	0.695 ± 0.070	2.44 ± 0.2	
	100		2.90	0.701	0.685	1.4	
		n = 10	2.30 ± 0.07	0.702 ± 0.022	0.697 ± 0.011	1.12 ± 0.2	
NS-TiO_2	0		15.78	0.973	0.710	10.9	
$MAPb(Br_xI_{1-x})_{3-y}Cl_y$		n = 10	15.20 ± 0.42	0.926 ± 0.052	0.701 ± 0.012	9.9 ± 0.9	1.58
	25		12.97	1.089	0.684	9.1	
		n = 2	12.00 ± 0.37	1.072 ± 0.024	0.680 ± 0.047	8.8 ± 0.5	1.74
	50		10.01	1.046	0.696	8.7	
		n = 9	9.89 ± 0.22	1.043 ± 0.012	0.684 ± 0.037	7.8 ± 0.8	1.87
	75		6.64	0.966	0.709	4.5	2.08
		n = 4	5.96 ± 0.71	0.934 ± 0.034	0.723 ± 0.041	4 ± 0.6	
	100		4.65	0.947	0.653	2.9	2.27
		n = 9	4.49 ± 0.15	0.934 ± 0.087	0.662 ± 0.019	2.8 ± 0.1	
NS-Al_2O_3	0		19.63	1.015	0.626	12.5	1.58
$MAPb(Br_xI_{1-x})_{3-y}Cl_y$		n = 5	19.45 ± 0.29	1.011 ± 0.004	0.614 ± 0.01	12.1 ± 0.4	
	50		10.23	1.082	0.403	4.5	1.88
		n = 5	10.2 ± 0.20	1.065 ± 0.025	0.391 ± 0.056	4.2 ± 0.5	
	100		3.92	1.389	0.586	3.2	2.29
		n = 5	3.92 ± 0.14	1.333 ± 0.069	0.602 ± 0.029	3.1 ± 0.3	
thin film	0	n = 5	14.76	1.077	0.699	11.1	
$MAPb(I_{1-x}Br_x)_{3-y}Cl_y$			14.58 ± 0.76	1.076 ± 0.030	0.694 ± 0.022	10.9 ± 0.5	
	50	n = 5	8.57	0.916	0.501	3.9	
			8.05 ± 0.48	1.020 ± 0.066	0.376 ± 0.073	3.1 ± 0.7	

[a]Short-circuit current, J_{sc}, open-circuit voltage, V_{oc}, fill factor, FF, photoconversion efficiency, η, and energy band gap, E_g (estimated from the absorption spectra) are included. The different solar cell configurations (NS and thin film), nature of the substrates (TiO_2 and Al_2O_3), and PS compositions ($MAPb(Br_xI_{1-x})_3$ and $MAPb(Br_xI_{1-x})_{3-y}Cl_y$, $0 \le x \le 1$) are evaluated. The data provided include the best performance device and the average of n devices prepared under the same conditions ($2 \le n \le 10$).

The highest efficiencies reported in the literature by using the one-step methodology reach the 15% for PS cells with Cl-doped films,[3,4] while a maximum efficiency of 9.7% has been achieved for Cl-free devices.[17] This observation points to the importance of exploiting the mixed-halide PS for the preparation of highly efficient devices. Despite the fact that the highest efficiencies reported for $MAPbI_3$ have been obtained so far by employing other deposition methods such as two-step sequential deposition[1,5] and sublimation[16] or using other hole-transport materials,[15] in this work, we have utilized the one-step spin coating deposition methodology to compare the effect of different halides for direct comparison with the one-step method used with Cl precursor.

dx.doi.org/10.1021/jz5006797 | J. Phys. Chem. Lett. 2014, 5, 1628−1635

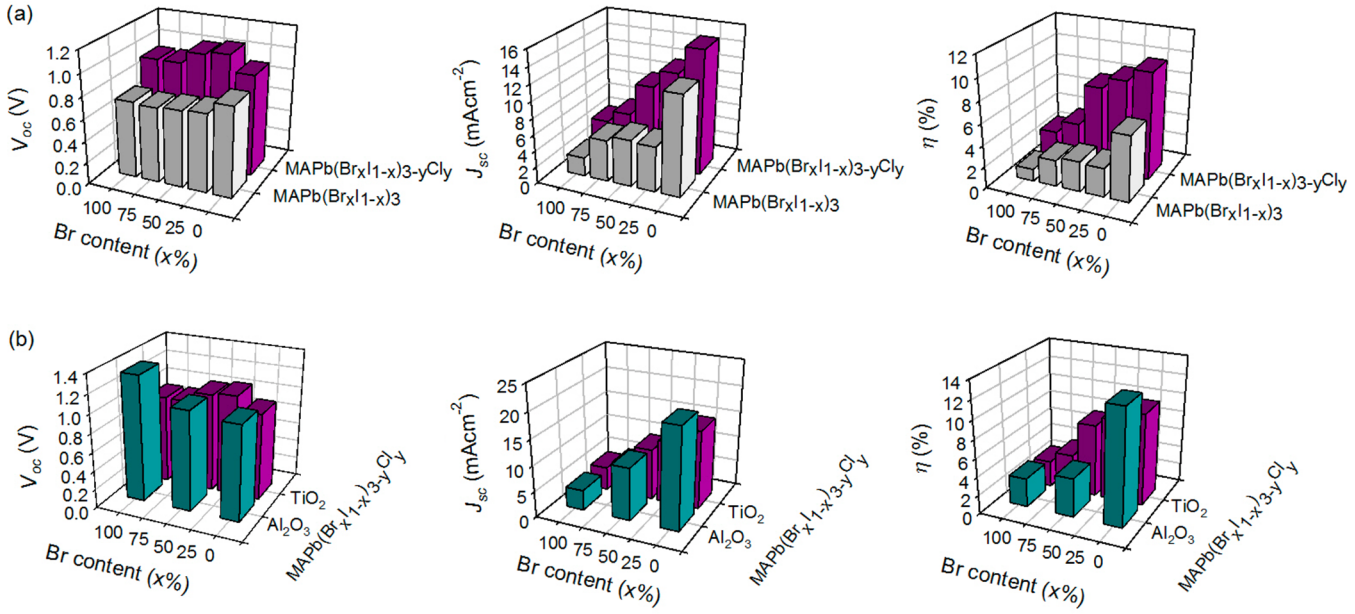

Figure 3. Open-circuit voltage, V_{oc}, short-circuit current, J_{sc}, and photoconversion efficiency, η, extracted from current−voltage curves under 1 sun illumination of several PS cells with different Br/I molar ratios are tested. (a) Combination of mixed halide PS, Cl free $MAPb(Br_xI_{1-x})_{3-y}$ versus trihalide PS $MAPb(Br_xI_{1-x})_{3-y}Cl_y$, ($0 \le x \le 1$), deposited on NS-$TiO_2$ substrates. (b) Comparison between two architectures NS-TiO_2 versus NS-Al_2O_3 substrates for $MAPbX_{3-y}Cl_y$ PS films. The data plotted correspond to the mean of a number "n" of working devices ($2 \le n \le 10$); see Table 1.

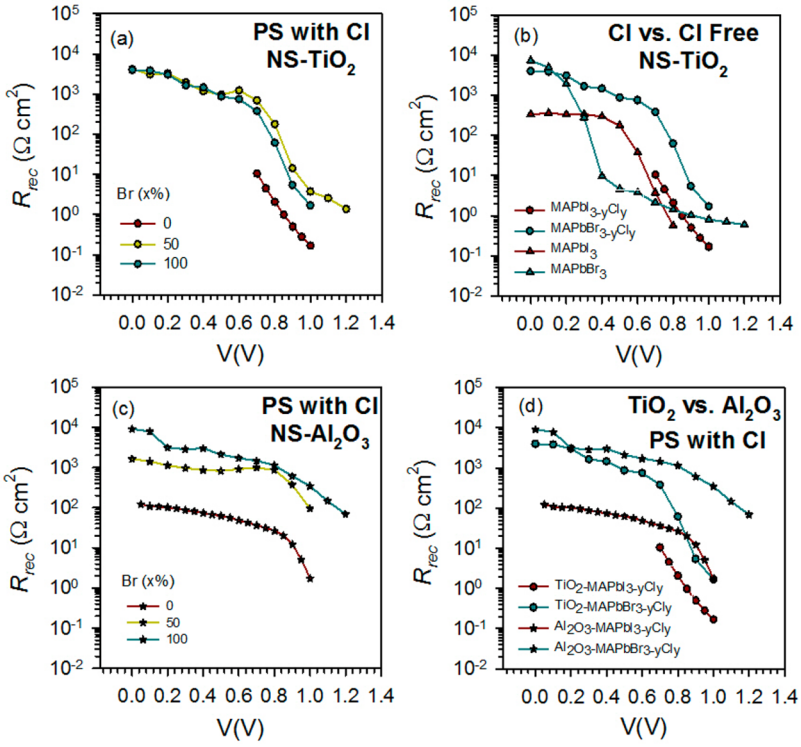

Figure 4. Recombination resistance at different applied bias extracted from the IS analysis of a mixed-halide-based PS solar cells with different Br/I molar ratios. Devices prepared from NS-TiO_2 substrates are represented by circles and triangles depending on the PS composition: with and without Cl, respectively. The NS-Al_2O_3 samples are represented by star symbols. (a) Trihalide perovskites $MAPb(Br_xI_{1-x})_{3-y}Cl_y$ devices on NS-TiO_2. (b) Comparison of samples with and without Cl prepared on NS-TiO_2. (c) Trihalide perovskites $MAPb(Br_xI_{1-x})_{3-y}Cl_y$ devices on NS-Al_2O_3 substrates. (d) Comparison of trihalide perovskites $MAPb(Br_xI_{1-x})_{3-y}Cl_y$ prepared on NS-TiO_2 and NS-Al_2O_3 substrates.

Although previous works found in the literature are focused on the thin-film devices based on bihalide structures (I−Cl, Br−Cl, or I−Br), we described here for the first time a combination of three halides (Cl, Br, and I) in complete PS devices. The good reproducibility showed in the photovoltaic parameters of the devices prepared by means of the three methodologies studied is noteworthy (Table 1). The IPCE onset of the prepared samples (Figure SI2 in the Supporting Information) shifts to shorter wavelengths with the Br addition,

dx.doi.org/10.1021/jz5006797 | J. Phys. Chem. Lett. 2014, 5, 1628−1635

which is correlated with the absorption measurements (Figure 1b); this trend is observed in all sample sets studied.

A comparative analysis of the photovoltaic parameters, V_{oc}, J_{sc}, and η, of the analyzed devices is shown in Figure 3. A remarkable increase in the V_{oc} and J_{sc} is observed for the films containing Cl, leading to a dramatic improvement in the efficiency (Figure 3a). The larger photocurrents can be attributed to the stronger absorption, as is evidenced in Figure SI1 in the Supporting Information. In the case of MAPb-$(Br_xI_{1-x})_{3-y}Cl_y$ sets grown onto NS-TiO_2 and NS-Al_2O_3, the later devices present higher efficiencies due to higher V_{oc} and J_{sc}, despite the lower FF, an exception for the PS device with Br 50% of content. The higher J_{sc} could be ascribed to the higher absorption of the samples grown on NS-Al_2O_3 substrates. (See Figure SI1 in the Supporting Information.)

The origin of V_{oc} in PS solar cells is an issue that is still unclear and is currently under study. However, a key aspect that has not yet been analyzed in depth is the influence of the recombination rate on the V_{oc}. It is well known that the recombination rate plays a major role in the V_{oc} values, as it has been analyzed, for example, for the dye-sensitized photovoltaic technology.[30,37] In this work, we analyze systematically, for the first time, the influence of the different recombination rates observed for PS samples containing different mixtures of halides on the photovoltage through an exhaustive characterization by means of IS.

IS technique is extensively used in Si solar cells,[38] extremely thin absorber (ETA) devices,[39−41] or solid dye-sensitized solar cells,[42,43] and, more recently, it has been proven to be suitable for the study of PS-based solar cells.[3,8,18,21,31−34] IS corresponds to a frequency-dependent technique that allows separating electrochemical processes that take place at different rates. The IS pattern of PS solar cells shows in most cases two characteristic features depending on the frequency range. At higher frequencies, the electrochemical processes at the contacts or at the PS−contact interface are observed.[21,31,32] In contrast, the features observed at low frequencies are related to the charge recombination processes.[21,31,32] The IS patterns of the different PS samples analyzed were fitted using an equivalent circuit model previously reported.[32]

The recombination resistances obtained from the IS experiments at different applied voltages under 1 sun illumination are plotted in Figure 4. As a general trend, two different slopes can be identified from the R_{rec} behavior. At low applied bias a gently decrease in the R_{rec} is noticed; however, a steeply sloped behavior is observed at high voltages. These differences can be attributed to a change in the recombination mechanisms. A hypothesis could be that charge recombination occurring at the surface interfaces is observed at low applied voltage, that is, recombination at the TiO_2 compact layer and spiro-OMeTAD layers, and the recombination processes taking place at the bulk PS are observed at high voltages. The determination of the exact physical processes involved in the charge recombination mechanisms of PS solar cells surpasses the scope of this work, and further research aimed to the elucidation of the abundant hidden aspects is required.

The R_{rec} values obtained for a series of PS samples supported on NS-TiO_2 substrates, corresponding to the generic formula MAPb$(Br_xI_{1-x})_{3-y}Cl_y$, are plotted in Figure 4a. From these results, it is clearly observed that the addition of Br induces a significant increase in the R_{rec}, thus having a beneficial effect on the cell performance. In fact, a clear correlation between a higher R_{rec} (lower recombination rate) and a higher V_{oc} is observed (Table 1), as it is clearly visible for the sample without Br. Note that for the samples with Br, the different J_{sc} also plays a role in V_{oc}, as V_{oc} increases with J_{sc},[30] making the samples with 100% I and 100% Br present similar V_{oc} despite the higher R_{rec} observed for the bromide sample. Additionally, Figure 4b compared these PS solar devices (MAPb$I_{3-y}Cl_y$ and MAPb-$Br_{3-y}Cl_y$) with their counterparts samples without Cl as $MAPbI_3$ and $MAPbBr_3$; the same study with 50% Br is represented in the Supporting Information (Figure SI3a). The IS analysis of two PS samples with identical Br content reveals that the presence of Cl induces a decrease in the recombination rate, thus enhancing the V_{oc} of the devices. (See Table 1.) This effect is even more significant when the Br content increases.

Furthermore, the results of the devices prepared with Cl-based PS films deposited onto NS-Al_2O_3 substrates in which the amount of Br was tuned, MAPb$(Br_xI_{1-x})_{3-y}Cl_y$ (x = 0, 0.5 and 1), are examined in Figure 4c. The R_{rec} values show the same behavior, while the Br content is increased, which is again reflected in an enhancement of the V_{oc}. The PS device with 100% Br presents lower recombination and achieves the highest V_{oc} value (1.389 V). Consequently, we claim that the addition of Br into the PS structure has a beneficial effect on the recombination rate. These results are in good agreement with those previously reported by Seok and coworkers.[15] The recombination rate for NS-Al_2O_3 devices is lower than that in the case of samples prepared on NS-TiO_2 substrates, independently of the Br/I ratio (Figure 4d for x = 0 and 1, and Figure SI3b in the Supporting Information for x = 0.5). This effect is reflected in the V_{oc} results, as illustrated in Figure 3b. The lower V_{oc} value obtained for MAPb$I_{3-y}Cl_y$ (0% of Br) on NS-TiO_2 in comparison with NS-Al_2O_3 is commonly attributed to the injection of electrons from PS into TiO_2. Injected electrons fill the high density of states (DOS) in the TiO_2, which can act as trap sites for the photogenerated free electrons.[19] According to this point of view, the addition of the TiO_2 states in the bandgap to the PS DOS will make the electrons at the Fermi level become lower and consequently decrease V_{oc} with respect to the Al_2O_3, which adds no states. But this argument requires that the number of stored electrons is the same in both systems, PS/TiO_2 and PS/Al_2O_3. However, the number of electrons critically depends on the recombination rate. The presence of an electronically active PS/TiO_2 interface can increase the recombination rate with respect PS/Al_2O_3 or induce different PS growth, affecting the recombination as it is observed in Figure 4d. In that case, the addition of TiO_2 states may lose relevance to explain the observed V_{oc}, which becomes dominated by kinetics.

Here we demonstrate a higher recombination rate for NS-TiO_2 PS films compared with those prepared using NS-Al_2O_3, both containing Cl (Figure 4d). However, a deeper study is needed to identify the origin of this effect, with the aim of clarifying whether the surface states of TiO_2 may induce a new recombination pathway and determining how the nature of the PS scaffold (TiO_2 or Al_2O_3) can affect to the PS growth or crystallinity, which could have, ultimately, a significant impact on the overall device performance. Therefore, we do believe that the identification of the main recombination pathways in PS solar cells is a mandatory step for good understanding of the functioning of these devices and their consequent optimization. Eventually, we have also noticed from the electrochemical characterization, as one would expect, that those devices showing lower R_{rec} present larger values of dark current (Figure SI4 in the Supporting Information).

dx.doi.org/10.1021/jz5006797 | J. Phys. Chem. Lett. 2014, 5, 1628−1635

Simultaneously to the IS study, we monitored the solar cell stability of MAPb$(Br_xI_{1-x})_{3-y}Cl_y$ PS, grown on NS-TiO_2 and in thin film configuration, to study the cell degradation as a function of the halide composition. The stability of PS solar devices is limited mainly due the ambient moisture because the alkylammonium salts are, in general, highly hygroscopic. We measured punctually the evolution of the photovoltaic parameters of the PS solar devices over time, and the samples were stored in a glovebox under a N_2 atmosphere and dark conditions between the measurements. Figure 5 plots the

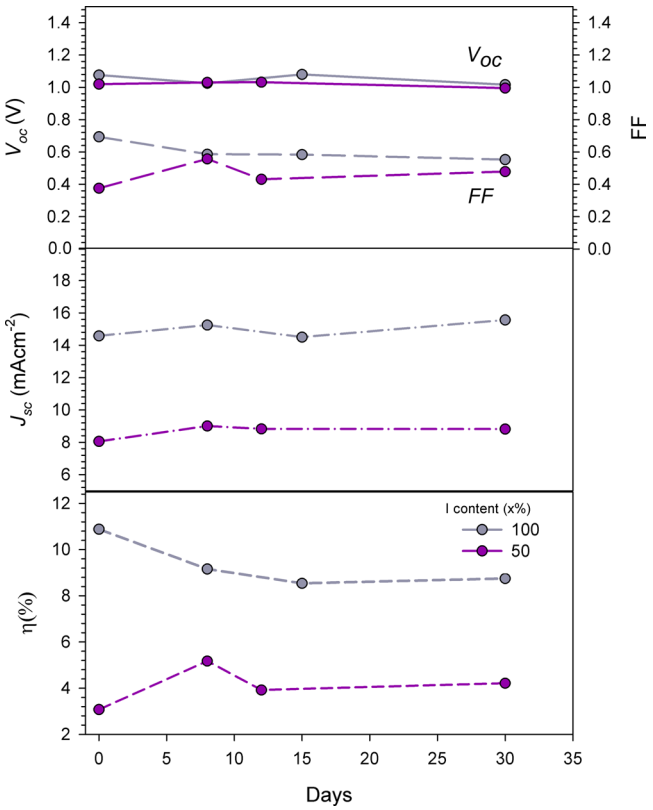

Figure 5. Time evolution of the photovoltaic parameters under 1 sun illumination for PS solar cells with a thin-film architecture and a mixture of three halide perovskites as MAPb$(I_{1-x}Br_x)_{3-y}Cl_y$, ($x = 0$ and $x = 0.5$). Samples were stored between measurements in the glovebox under dark conditions.

evolution of photovoltaics parameters with time for thin-film architecture. As previously reported,[15] the insertion of Br into the PS structure produces a beneficial effect in the cell stability. Those cells without Br present an efficiency drop of 20% 30 days after their preparation, which is ascribed mainly to a decrease in the FF. On the contrary, the equimolar Br/I devices show a significant enhancement of the photoconversion efficiency (37%). This improvement could be a consequence of the rearrangement of the PS 3D configuration over time. In particular, the efficiency improvement could be attributed to the insertion of the smaller Br anions, thus leading to a more compact PS structure in which the degradation of the MA cation is prevented.[15] Therefore, a deeper analysis including microstructural and crystallographic studies must be performed to elucidate the origin of this observation. The cell efficiencies of the samples grown on NS-TiO_2 substrates are plotted in Figure SI5 in the Supporting Information and point similarly to an increase in the stability cell when the Br is inserted into the PS structure; hence, this effect seems to be a common denominator regardless of the cell architecture.

In summary, the combination of ternary mixtures of halides (Cl, Br, and I) for the preparation of PS solar cells by exploiting different cell architectures has been exhaustively analyzed. We report different easy-to-fabricate solution-processed band-gap-tailored materials and, as far as we know, we described for the first time a trihalide thin-film solar cell. This work has mainly focused on the recombination characteristics as a function of the halide content and device architecture (NS-TiO_2 and NS-Al_2O_3) by means of a systematic analysis by IS. Particular trends have been observed for the devices tested, which allow us to confirm that the charge recombination is reduced when: (i) the Br/I ratio is increased and being specially more pronounced when NS-Al_2O_3 substrates are employed; (ii) the Cl is incorporated in the PS precursor solution; and (iii) the NS-Al_2O_3 substrates are used as an efficient PS scaffold. A clear correlation between the decrease in the recombination rate and the enhancement of the V_{oc} was observed; therefore, an improvement of the overall cell performance promoted by inhibiting the recombination mechanisms has been validated. In addition, the study of the cell stabilities carried out in this work revealed an enhanced stability for those PS samples containing Br. The exact physical mechanisms that have promoted these changes in recombination processes among the different cells analyzed in this work are under current study. Very recently, it has been pointed out that the presence of nanostructured TiO_2 affects the crystalline properties of synthesized PS, affecting the photoluminescence behavior.[44−46] In addition, an effect on recombination should be also expected, but further research is needed to correlate the observed changes in recombination with the crystalline properties of PS samples.

These results point out the importance of a complete characterization of the recombination processes in the PS solar cells to fully understand the physical mechanisms that rule the PS-based photovoltaic technology and to evolve to more efficient and stable devices. It is noteworthy that the most significant improvements of the cell efficiencies promoted in other photovoltaic technologies, for example, dye-sensitized solar cells, arose from the partial inhibition and understanding of the charge recombination processes.

■ ASSOCIATED CONTENT

Supporting Information

Methods, light absorption for MAPb$(I_{1-x}Br_x)_{3-y}Cl_y$ samples on NS-TiO_2 and NS-Al_2O_3, incident photon to current efficiency (IPCE), recombination resistance, $J-V$ curves under dark illumination conditions, and stability. This material is available free of charge via the Internet at http://pubs.acs.org.

■ AUTHOR INFORMATION

Corresponding Author

*E-mail: sero@uji.es.

Notes

The authors declare no competing financial interest.

■ ACKNOWLEDGMENTS

This work was supported by Generalitat Valenciana (ISIC/2012/008) and Universitat Jaume I project 12I361.01/1. We acknowledge Prof. J. Bisquert for the fruitful discussion on the topics of the manuscript.

REFERENCES

(1) Burschka, J.; Pellet, N.; Moon, S.-J.; Humphry-Baker, R.; Gao, P.; Nazeeruddin, M. K.; Graetzel, M. Sequential Deposition as a Route to High-Performance Perovskite-Sensitized Solar Cells. *Nature* **2013**, *499*, 316−319.

(2) Liu, M.; Johnston, M. B.; Snaith, H. J. Efficient Planar Heterojunction Perovskite Solar Cells by Vapour Deposition. *Nature* **2013**, *501*, 395−398.

(3) Wang, J. T.-W.; Ball, J. M.; Barea, E. M.; Abate, A.; Alexander-Webber, J. A.; Huang, J.; Saliba, M.; Mora-Sero, I.; Bisquert, J.; Snaith, H. J.; et al. Low-Temperature Processed Electron Collection Layers of Graphene/TiO2 Nanocomposites in Thin Film Perovskite Solar Cells. *Nano Lett.* **2014**, *14*, 724−730.

(4) Wojciechowski, K.; Saliba, M.; Leijtens, T.; Abate, A.; Snaith, H. J. Sub-150°C Processed Meso-Superstructured Perovskite Solar Cells with Enhanced Efficiency. *Energy Environ. Sci.* **2014**, *7*, 1142−1147.

(5) Liu, D.; Kelly, T. L. Perovskite Solar Cells with a Planar Heterojunction Structure Prepared Using Room-Temperature Solution Processing Techniques. *Nat. Photonics* **2014**, *8*, 133−138.

(6) Park, N.-G. Organometal Perovskite Light Absorbers Toward a 20% Efficiency Low-Cost Solid-State Mesoscopic Solar Cell. *J. Phys. Chem. Lett.* **2013**, *4*, 2423−2429.

(7) Snaith, H. J. Perovskites: The Emergence of a New Era for Low-Cost, High-Efficiency Solar Cells. *J. Phys. Chem. Lett.* **2013**, *4*, 3623−3630.

(8) Kumar, M. H.; Yantara, N.; Dharani, S.; Graetzel, M.; Mhaisalkar, S.; Boix, P. P.; Mathews, N. Flexible, Low-Temperature, Solution Processed ZnO-Based Perovskite Solid State Solar Cells. *Chem. Commun.* **2013**, *49*, 11089−11091.

(9) Docampo, P.; Ball, J. M.; Darwich, M.; Eperon, G. E.; Snaith, H. J. Efficient Organometal Trihalide Perovskite Planar-Heterojunction Solar Cells on Flexible Polymer Substrates. *Nat. Commun.* **2013**, *4*, 2761.

(10) Mitzi, D. B. Synthesis, Structure, and Properties of Organic-Inorganic Perovskites and Related Materials. In *Progress in Inorganic Chemistry*; Karlin, K. D., Ed.; John Wiley & Sons: Hoboken, NJ, 2007; Vol. *48*.

(11) Stoumpos, C. C.; Malliakas, C. D.; Kanatzidis, M. G. Semiconducting Tin and Lead Iodide Perovskites with Organic Cations: Phase Transitions, High Mobilities, and Near-Infrared Photoluminescent Properties. *Inorg. Chem.* **2013**, *52*, 9019−9038.

(12) Eperon, G. E.; Stranks, S. D.; Menelaou, C.; Johnston, M. B.; Herz, L. M.; Snaith, H. J. Formamidinium Lead Trihalide: a Broadly Tunable Perovskite for Efficient Planar Heterojunction Solar Cells. *Energy Environ. Sci.* **2014**, *7*, 982−988.

(13) Edri, E.; Kirmayer, S.; Cahen, D.; Hodes, G. High Open-Circuit Voltage Solar Cells Based on Organic−Inorganic Lead Bromide Perovskite. *J. Chem. Phys. Lett.* **2013**, *4*, 897−902.

(14) Edri, E.; Kirmayer, S.; Kulbak, M.; Hodes, G.; Cahen, D. Chloride Inclusion and Hole Transport Material Doping to Improve Methyl Ammonium Lead Bromide Perovskite-Based High Open-Circuit Voltage Solar Cells. *J. Chem. Phys. Lett.* **2014**, *5*, 429−433.

(15) Noh, J. H.; Im, S. H.; Heo, J. H.; Mandal, T. N.; Seok, S. I. Chemical Management for Colorful, Efficient, and Stable Inorganic−Organic Hybrid Nanostructured Solar Cells. *Nano Lett.* **2013**, *13*, 1764−1769.

(16) Malinkiewicz, O.; Yella, A.; Lee, Y. H.; Espallargas, G. M.; Graetzel, M.; Nazeeruddin, M. K.; Bolink, H. J. Perovskite Solar Cells Employing Organic Charge-Transport Layers. *Nat. Photonics* **2014**, *8*, 128−132.

(17) Kim, H.-S.; Lee, C.-R.; Im, J.-H.; Lee, K.-B.; Moehl, T.; Marchioro, A.; Moon, S.-J.; Humphry-Baker, R.; Yum, J.-H.; Moser, J. E.; Graetzel, M.; et al. Lead Iodide Perovskite Sensitized All-Solid-State Submicron Thin Film Mesoscopic Solar Cell with Efficiency Exceeding 9%. *Sci. Rep.* **2012**, *2*, 591.

(18) Kim, H.-S.; Mora-Sero, I.; Gonzalez-Pedro, V.; Fabregat-Santiago, F.; Juarez-Perez, E. J.; Park, N.-G.; Bisquert, J. Mechanism of Carrier Accumulation in Perovskite Thin-Absorber Solar Cells. *Nat. Commun.* **2013**, *4*, 2242.

(19) Lee, M. M.; Teuscher, J.; Miyasaka, T.; Murakami, T. N.; Snaith, H. J. Efficient Hybrid Solar Cells Based on Meso-Superstructured Organometal Halide Perovskites. *Science* **2012**, *338*, 643−647.

(20) Ball, J. M.; Lee, M. M.; Hey, A.; Snaith, H. J. Low-Temperature Processed Meso-Superstructured to Thin-Film Perovskite Solar Cells. *Energy Environ. Sci.* **2013**, *6*, 1739−1743.

(21) Gonzalez-Pedro, V.; Juarez-Perez, E. J.; Arsyad, W.-S.; Barea, E. M.; Fabregat-Santiago, F.; Mora-Sero, I.; Bisquert, J. General Working Principles of $CH_3NH_3PbX_3$ Perovskite Solar Cells. *Nano Lett.* **2014**, *14*, 888−893.

(22) Edri, E.; Kirmayer, S.; Henning, A.; Mukhopadhyay, S.; Gartsman, K.; Rosenwaks, Y.; Hodes, G.; Cahen, D. Why Lead Methylammonium Tri-Iodide Perovskite-Based Solar Cells Require a Mesoporous Electron Transporting Scaffold (but Not Necessarily a Hole Conductor). *Nano Lett.* **2014**, *14*, 1000−1004.

(23) Colella, S.; Mosconi, E.; Fedeli, P.; Listorti, A.; Gazza, F.; Orlandi, F.; Ferro, P.; Besagni, T.; Rizzo, A.; Calestani, G.; et al. $MAPbI_{3-x}Cl_x$ Mixed Halide Perovskite for Hybrid Solar Cells: The Role of Chloride as Dopant on the Transport and Structural Properties. *Chem. Mater.* **2013**, *25*, 4613−4618.

(24) Stranks, S. D.; Eperon, G. E.; Grancini, G.; Menelaou, C.; Alcocer, M. J. P.; Leijtens, T.; Herz, L. M.; Petrozza, A.; Snaith, H. J. Electron-Hole Diffusion Lengths Exceeding 1 Micrometer in an Organometal Trihalide Perovskite Absorber. *Science* **2013**, *342*, 341−344.

(25) Bi, D.; Yang, L.; Boschloo, G.; Hagfeldt, A.; Johansson, E. M. J. Effect Different Hole Transport Materials on Recombination in $CH_3NH_3PbI_3$ Perovskite-Sensitized Mesoscopic Solar Cells. *J. Phys. Chem. Lett.* **2013**, *4*, 1532−1536.

(26) Zhao, Y.; Nardes, A. M.; Zhu, K. Solid-State Mesostructured Perovskite $CH_3NH_3PbI_3$ Solar Cells: Charge Transport, Recombination, and Diffusion Length. *J. Phys. Chem. Lett.* **2014**, *5*, 490−494.

(27) Zhao, Y.; Zhu, K. Charge Transport and Recombination in Perovskite $(CH_3NH_3)PbI_3$ Sensitized TiO_2 Solar Cells. *J. Phys. Chem. Lett.* **2013**, *4*, 2880−2884.

(28) Wehrenfennig, C.; Eperon, G. E.; Johnston, M. B.; Snaith, H. J.; Herz, L. M. High Charge Carrier Mobilities and Lifetimes in Organolead Trihalide Perovskites. *Adv. Mater.* **2014**, *26*, 1584−1589.

(29) Xing, G.; Mathews, N.; Sun, S.; Lim, S. S.; Lam, Y. M.; Grätzel, M.; Mhaisalkar, S.; Sum, T. C. Long-Range Balanced Electron- and Hole-Transport Lengths in Organic-Inorganic $CH_3NH_3PbI_3$. *Science* **2013**, *342*, 344−347.

(30) Fabregat-Santiago, F.; Garcia-Belmonte, G.; Mora-Sero, I.; Bisquert, J. Characterization of Nanostructured Hybrid and Organic Solar Cells by Impedance Spectroscopy. *Phys. Chem. Chem. Phys.* **2011**, *13*, 9083−9118.

(31) Dualeh, A.; Moehl, T.; Tétreault, N.; Teuscher, J.; Gao, P.; Nazeeruddin, M. K.; Grätzel, M. Impedance Spectroscopic Analysis of Lead Iodide Perovskite-Sensitized Solid-State Solar Cells. *ACS Nano* **2013**, *8* (1), 362−373.

(32) Juarez-Perez, E. J.; Wußler, M.; Fabregat-Santiago, F.; Lakus-Wollny, K.; Mankel, E.; Mayer, T.; Jaegermann, W.; Mora-Sero, I. Role of the Selective Contacts in the Performance of Lead Halide Perovskite Solar Cells. *J. Phys. Chem. Lett.* **2014**, *5*, 680−685.

(33) Kim, H.-S.; Lee, J.-W.; Yantara, N.; Boix, P. P.; Kulkarni, S. A.; Mhaisalkar, S.; Gratzel, M.; Park, N.-G. High Efficiency Solid-State Sensitized Solar Cell-Based on Submicrometer Rutile TiO_2 Nanorod and $CH_3NH_3PbI_3$ Perovskite Sensitizer. *Nano Lett.* **2013**, *16*, 2412−2417.

(34) Christians, J. A.; Fung, R. C. M.; Kamat, P. V. An Inorganic Hole Conductor for Organo-Lead Halide Perovskite Solar Cells. Improved Hole Conductivity with Copper Iodide. *J. Am. Chem. Soc.* **2013**, *136*, 758−764.

(35) Schulz, P.; Edri, E.; Kirmayer, S.; Hodes, G.; Cahen, D.; Kahn, A. Interface Energetics in Organo-Metal Halide Perovskite-Based Photovoltaic Cells. *Energy Environ. Sci.* **2014**, *7*, 1377−1381.

(36) Kojima, A.; Teshima, K.; Shirai, Y.; Miyasaka, T. Organometal Halide Perovskites as Visible-Light Sensitizers for Photovoltaic Cells. *J. Am. Chem. Soc.* **2009**, *131*, 6050−6051.

(37) Marinado, T.; Nonomura, K.; Nissfolk, J.; Karlsson, M. K.; Hagberg, D. P.; Sun, L.; Mori, S.; Hagfeldt, A. How the Nature of Triphenylamine-Polyene Dyes in Dye-Sensitized Solar Cells Affects the Open-Circuit Voltage and Electron Lifetimes. *Langmuir* **2009**, *26*, 2592−2598.
(38) Mora-Sero, I.; Garcia-Belmonte, G.; Boix, P. P.; Vazquez, M. A.; Bisquert, J. Impedance Spectroscopy Characterisation of Highly Efficient Silicon Solar Cells Under Different Light Illumination Intensities. *Energy Environ. Sci.* **2009**, *2* (6), 678−686.
(39) Boix, P. P.; Larramona, G.; Jacob, A.; Delatouche, B.; Mora-Seró, I.; Bisquert, J. Hole Transport and Recombination in All-Solid Sb2S3-Sensitized TiO_2 Solar Cells Using CuSCN As Hole Transporter. *J. Phys. Chem. Lett.* **2011**, *116*, 1579−1587.
(40) Boix, P. P.; Lee, Y. H.; Fabregat-Santiago, F.; Im, S. H.; Mora-Sero, I.; Bisquert, J.; Seok, S. I. From Flat to Nanostructured Photovoltaics: Balance between Thickness of the Absorber and Charge Screening in Sensitized Solar Cells. *ACS Nano* **2011**, *6*, 873−880.
(41) Mora-Sero, I.; Gimenez, S.; Fabregat-Santiago, F.; Azaceta, E.; Tena-Zaera, R.; Bisquert, J. Modeling and Characterization of Extremely Thin Absorber (Eta) Solar Cells Based on ZnO Nanowires. *Phys. Chem. Chem. Phys.* **2011**, *13*, 7162−7169.
(42) Dualeh, A.; Moehl, T.; Nazeeruddin, M. K.; Grätzel, M. Temperature Dependence of Transport Properties of Spiro-MeOTAD as a Hole Transport Material in Solid-State Dye-Sensitized Solar Cells. *ACS Nano* **2013**, *7*, 2292−2301.
(43) Fabregat-Santiago, F.; Bisquert, J.; Cevey, L.; Chen, P.; Wang, M.; Zakeeruddin, S. M.; Grätzel, M. Electron Transport and Recombination in Solid-State Dye Solar Cell with Spiro-OMeTAD as Hole Conductor. *J. Am. Chem. Soc.* **2009**, *131*, 558−562.
(44) Choi, J. J.; Yang, X.; Norman, Z. M.; Billinge, S. J. L.; Owen, J. S. Structure of Methylammonium Lead Iodide Within Mesoporous Titanium Dioxide: Active Material in High-Performance Perovskite Solar Cells. *Nano Lett.* **2013**, *14*, 127−133.
(45) Roiati, V.; Colella, S.; Lerario, G.; De Marco, L.; Rizzo, A.; Listorti, A.; Gigli, G. Investigating Charge Dynamics in Halide Perovskite-Sensitized Mesostructured Solar Cells. *Energy Environ. Sci.* **2014**, DOI: 10.1039/C3EE43991G.
(46) Roiati, V.; Mosconi, E.; Listorti, A.; Colella, S.; Gigli, G.; De Angelis, F. Stark Effect in Perovskite/TiO_2 Solar Cells: Evidence of Local Interfacial Order. *Nano Lett.* **2014**, *14*, 2168−2174.